© 2014. Published by The Company of Biologists Ltd | Journal of Cell Science (2014) 127, 2528–2541 doi:10.1242/jcs.144345

RESEARCH ARTICLE

Tight coupling between nucleus and cell migration through the perinuclear actin cap

Dong-Hwee Kim[1,2,*], Sangkyun Cho[2] and Denis Wirtz[1,2,3,*]

ABSTRACT

Although eukaryotic cells are known to alternate between 'advancing' episodes of fast and persistent movement and 'hesitation' episodes of low speed and low persistence, the molecular mechanism that controls the dynamic changes in morphology, speed and persistence of eukaryotic migratory cells remains unclear. Here, we show that the movement of the interphase nucleus during random cell migration switches intermittently between two distinct modes – rotation and translocation – that follow with high fidelity the sequential rounded and elongated morphologies of the nucleus and cell body, respectively. Nuclear rotation and translocation mediate the stop-and-go motion of the cell through the dynamic formation and dissolution, respectively, of the contractile perinuclear actin cap, which is dynamically coupled to the nuclear lamina and the nuclear envelope through LINC complexes. A persistent cell movement and nuclear translocation driven by the actin cap are halted following the disruption of the actin cap, which in turn allows the cell to repolarize for its next persistent move owing to nuclear rotation mediated by cytoplasmic dynein light intermediate chain 2.

KEY WORDS: Actin cap, Nuclear migration, Cell migration

INTRODUCTION

A motile *E. coli* alternates between fast persistent moves mediated by its flagella dominantly rotating counterclockwise and tumbling events mediated by the flagella transiently rotating clockwise (Berg, 1993). Similarly, a wide range of eukaryotic cells also alternate between 'advancing' episodes of fast and persistent movements and 'hesitation' episodes of low speed and low persistence. However, the molecular mechanism that controls the dynamic changes in morphology, speed and persistence of migratory cells remains unclear.

During random mesenchymal migration (i.e. no chemotactic gradients), cells continuously change their morphology, dynamically switching between elongated and round morphology (Köppen et al., 2006). Maintaining cell polarity by properly positioning the nucleus is necessary for mesenchymal cell migration, which is driven by repeated cycles of polarization, protrusion, translocation and retraction of the cell (Bretscher, 2008; Horwitz and Webb, 2003; Morris, 2000; Petrie et al., 2009). Although nuclear movements mediated by microtubule-dependent processes have been studied extensively (Cadot et al., 2012; Lee et al., 2005; Levy and Holzbaur, 2008; Umeshima et al., 2007; Wilson and Holzbaur, 2012), recent work has revealed that actin filaments are also involved in nuclear dynamics in migrating cells (Gomes et al., 2005) through specific connections between the nuclear envelope and the actin cytoskeleton (Starr and Fridolfsson, 2010). In polarized cells, F-actin is involved in initial symmetry-disrupting processes that rapidly respond to external stimuli; microtubules stabilize the asymmetry generated by actin filament dynamics (Li and Gundersen, 2008). In particular, transmembrane actin-associated nuclear (TAN) lines assembled with cytoplasmic actin filaments and LINC (linkers of nucleoskeleton and cytoskeleton) complex proteins nesprin-2 giant (nesprin-2G, the largest isoform encoded by the *Syne2* gene) and SUN2 have been found to enable reward movement of the nucleus in migrating fibroblasts in the wound healing assay (Luxton et al., 2010).

Recently, we characterized highly ordered actomyosin filament bundles that tightly cover the apical surfaces of the interphase nucleus and specifically bind the nuclear envelope and the nuclear lamina through LINC complexes in a wide range of adherent cells, termed the perinuclear actin cap (or actin cap) (Khatau et al., 2009; Kim et al., 2013). The actin-cap fibers and their terminating focal adhesions act as key components of the physical pathway that converts extracellular stimuli into intracellular signals (Kim et al., 2013; Kim et al., 2012). As cell migration involves continuous mechanosensation, and various physiological and pathological processes – such as cancer metastasis and embryonic development – are highly dependent on cell motility (Chaffer and Weinberg, 2011; Gupta and Massagué, 2006; Thiery et al., 2009; Wirtz et al., 2011), we hypothesized that the actin cap would regulate cell migration.

Here, our results indicate that the dynamic formation and dissolution of the actin cap tightly controls the timing and occurrence of fast persistence moves in fibroblast migration. Furthermore, this study reveals that the translocation and rotation of the interphase nucleus are regulated by the dynamic attachment of the actin cap to the nuclear envelope via KASH-SUN interactions in the perinuclear space between the inner and outer nuclear membranes.

RESULTS

The actin cap controls cell migration

During random migration, mesenchymal cells such as mouse embryonic fibroblasts (MEFs) continuously change their morphology, dynamically switching between an elongated and a rounded shape. We have recently shown that cell shape controls nuclear shape through the formation of the actin cap (Khatau et al., 2009), which is organized at the apical surface of the nucleus (Fig. 1A and supplementary material Movie 1). In the absence of chemotactic gradients, the migration of adherent cells,

[1]Johns Hopkins Physical Sciences – Oncology Center, The Johns Hopkins University, Baltimore, MD 21218, USA. [2]Department of Chemical and Biomolecular Engineering, The Johns Hopkins University, Baltimore, MD 21218, USA. [3]Departments of Pathology and Oncology and Sydney Kimmel Comprehensive Cancer Center, The Johns Hopkins School of Medicine, Baltimore, MD 21205, USA.

*Authors for correspondence (narrkim@jhu.edu, wirtz@jhu.edu)

Received 10 October 2013; Accepted 10 March 2014

Journal of Cell Science

Journal of Cell Science (2014) 127, 2528–2541 doi:10.1242/jcs.144345

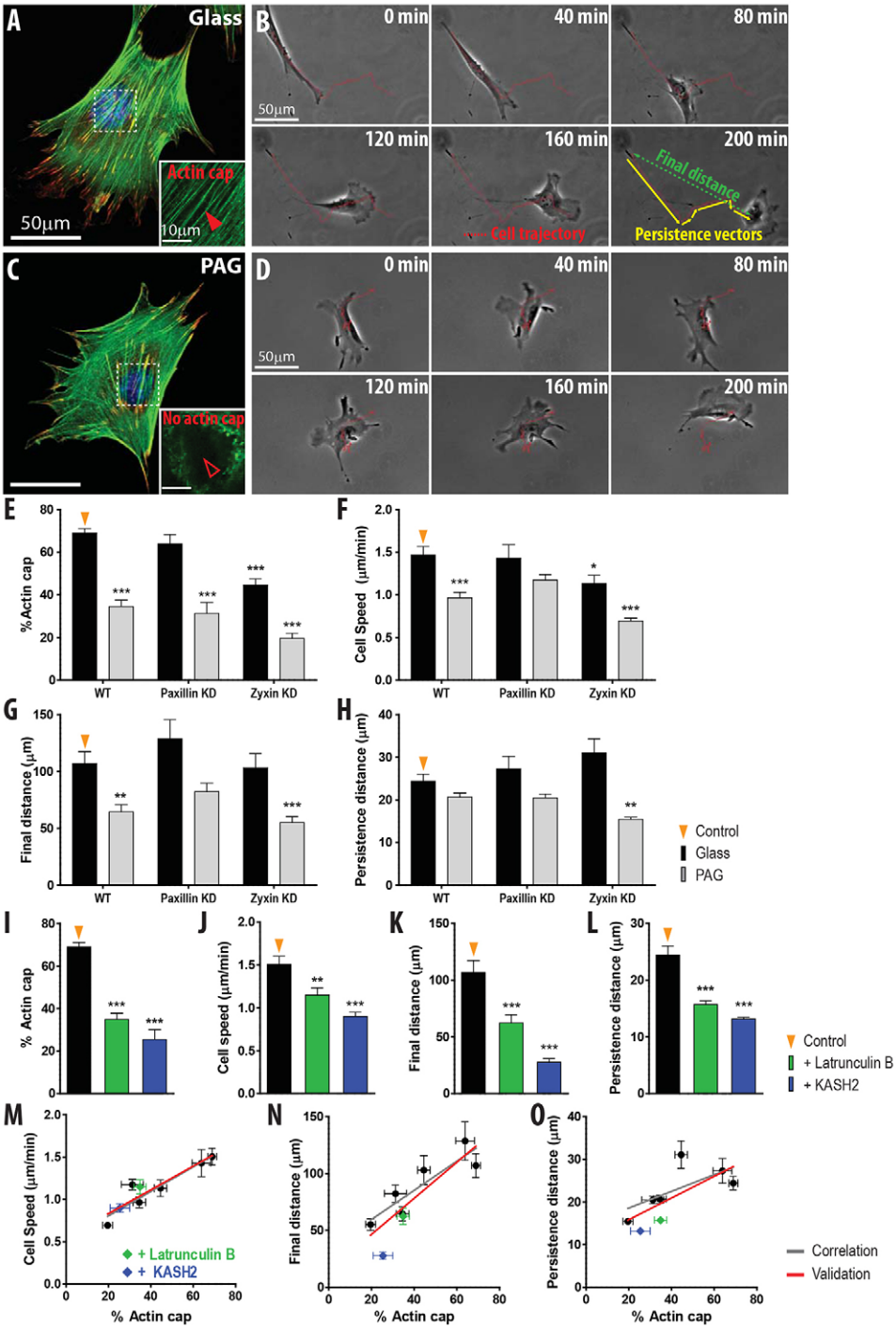

Fig. 1. The role of the actin cap in cell migration. (A–D) Differential formation of the actin cap and migration of MEFs lying on glass (A,B) or polyacrylamide hydrogel (C,D). DAPI-stained nucleus (blue), actin filaments (green) and vinculin-marked focal adhesions (red) of MEFs reveal that specific disruption of the actin cap does not affect the organization of basal actin fibers (A versus C). Cell trajectories (red), decomposed into persistence vectors (yellow) connecting episodes of non-persistent motion, and final distance (green) were estimated from 8 h movies (B). MEFs with a disrupted actin cap moved less persistently than actin-cap-forming MEFs (B versus D). (E–H) Proportion of cells showing an actin cap (E), cell speed (F), final distance (G) and persistence distance (H) in response to changes in substrate compliance (black, glass; gray, polyacrylamide hydrogel) and shRNA-induced depletion of focal adhesion proteins paxillin and zyxin. (I–L) Proportion of cells featuring an actin cap (I), cell speed (J), final distance (K) and persistence distance (L) for control cells, for cells treated with latrunculin B (green) and for cells transfected with EGFP-KASH2 (blue). (M–O) Correlative analysis between the formation of actin cap and cell migration. Straight lines obtained by linear regression represent overall trends of correlations. Corresponding Pearson's correlation coefficients *r* values are 0.93, 0.89 and 0.68 for gray (correlation with data obtained by changes in substrate compliance and depletion of focal adhesion proteins), and 0.93, 0.86 and 0.72 for red (validation with latrunculin B treatment and KASH2 transfection), respectively. Over 300 cells were analyzed to determine the fraction of cells forming an actin cap (E,I) and over 50 cells were monitored to measure the descriptors of cell motility (F–H,J–L) per condition. Panel E was adapted from Kim et al., 2012; and panels F–H were adapted from Kim and Wirtz, 2013a, Kim and Wirtz, 2013b.

including fibroblasts, endothelial cells and myoblasts, which can form an organized actin cap (Kim et al., 2013), resembles a persistent random-walk that consists of intermittent highly persistent fast moves and slow moves of low persistence (Fig. 1B and supplementary material Movie 2). Confirming the previous results that selective disruption of the actin cap could be achieved by modulating substrate compliance without affecting the organization of basal actin stress fibers (Kim et al., 2012), a MEF placed on soft polyacrylamide hydrogel (PAG) substrates did not form an actin cap while the basal actin fibers remained intact (Fig. 1C). These cells, which lack an actin cap, moved significantly more slowly and less persistently than cells on control stiff substrates (Fig. 1D and supplementary material Movie 3). Therefore, we asked whether the actin cap would direct cell migration: its absence would slow down cell migration, whereas its presence would enhance cell migration.

To assess systematically the role of the actin cap in cell migration, we first estimated the fraction of cells that formed an organized actin cap, mean speed, final distance (the end-to-end displacement during the observation of cell migration) and the persistence distance (mean distance travelled during correlated persistent moves) of control cells and cells depleted of major

Journal of Cell Science

focal adhesion proteins (e.g. paxillin and zyxin). The alteration of mechanical compliance of substrates as well as the depletion of focal-adhesion proteins are known to modulate cell migration through changes in focal adhesion size (Fig. 1E–H, replotted from Kim et al., 2012; Kim and Wirtz, 2013a; Kim and Wirtz, 2013b). We analyzed the extent of correlation between the formation of the actin cap and descriptors of cell migration. Here, we found that the cells that formed an actin cap moved more rapidly and more persistently (gray lines, Fig. 1M–O).

To go beyond a correlative assessment and establish the causality between the formation of actin cap and cell motility, the actin cap was specifically dismantled by treating cells with a low dose (60 nM) of the actin-depolymerizing drug latrunculin B (green, Fig. 1I) because this treatment does not affect the organization of conventional basal stress fibers (Kim et al., 2012) and does not significantly change gene expression (supplementary material Fig. S1). As predicted by our model of actin-cap-based cell motility, specific elimination of the actin cap reduced cell speed and persistence (green, Fig. 1J–L). The actin cap was also specifically eliminated by transfecting cells with the EGFP-KASH2 construct (blue, Fig. 1I), which disrupts KASH-SUN connections in the perinuclear space of the nuclear envelope (Stewart-Hutchinson et al., 2008). As predicted, these cells also showed significantly lower speed and persistence than control cells (blue, Fig. 1J–L) and their changes were tightly predicted by the previous correlative analysis (red lines, Fig. 1M–O).

To further confirm that the actin cap controls cell migration through actin-cap attachment to the nuclear envelope via KASH–SUN interactions, we compared the speed and persistence of nesprin-2G-depleted C2C12 mouse myoblasts cells and control cells transfected with a scrambled construct (supplementary material Fig. S2). As nesprin-2G has been shown to colocalize with actin fibers in the perinuclear region and to regulate nuclear motion (Borrego-Pinto et al., 2012; Luxton et al., 2010), the depletion of this LINC protein significantly reduced the fraction of cells that formed an actin cap (supplementary material Fig. S2A,B). Once again, the elimination of the actin cap, this time by depletion of nesprin-2G, reduced cell speed and persistence, as predicted above (supplementary material Fig. S2C). Together, these mechanical (Fig. 1A–D), pharmacological (Fig. 1I–O) and genetic (Fig. 1E–O and supplementary material Fig. S2) manipulations indicate that the tight connection of the actin cap to the nucleus is a crucial mediator of cell migration.

The nucleus displays mutually exclusive rotation and translocation

As cell migration is closely related to the differential formation of the actin cap (Fig. 1) and the actin cap regulates nuclear morphology through LINC complexes (Khatau et al., 2009), we asked whether the nucleus also showed two distinct morphologies and migratory modes during cell migration. To test this hypothesis, we first monitored the morphology and movements of the interphase nucleus of a randomly migrating cell (Fig. 2A and supplementary material Movie 4). Morphological analysis of the nucleus revealed that the time-dependent changes in size (i.e. projected area of the nucleus) and shape of the nucleus were tightly related (green and blue curves, Fig. 2B), whereas the instantaneous movement of the nuclear centroid (i.e. nuclear speed) was inversely correlated with both size and shape of the nucleus (red versus green and blue curves, Fig. 2B). The nucleus alternatively switched between a small elongated shape and a large rounded shape, which corresponded to rapid and slow nuclear migration, respectively (Fig. 2B). These results were confirmed by systematic correlative analysis among nuclear size, nuclear shape factor and nuclear speed (supplementary material Fig. S3A,B). We note that the nuclear volume measured by time-dependent swept-field confocal microscopy was approximately constant during the aforementioned morphological transitions (supplementary material Fig. S3C,D).

Next, we hypothesized that the nucleus could move in fundamentally different ways depending on nuclear morphology since changes in nuclear morphology occurred at a critical nuclear size that delineated the fast moving phase of the nucleus from its slowly moving phase (Fig. 2C,D). To test this notion, we transfected cells with EGFP-histone H2B to monitor nuclear morphology and nuclear displacements simultaneously. Consistent with the previous result (Fig. 2A–D), elongated nuclei (marked by A and B) were smaller and moved more rapidly than the rounded nucleus (marked by C), which was relatively large and moved slowly (Fig. 2E–I). We also noticed that the rounded nucleus rotated intermittently (Fig. 2E and supplementary material Movie 5) and net longitudinal displacements of the nuclear centroid were consistently smaller than for elongated nuclei (see the distribution of instantaneous displacements, inset of Fig. 2H). By contrast, elongated nuclei underwent fast translocation with no or little rotation. These results indicated that the slow migration of a rounded and large nucleus coincided with effective nuclear rotation accompanied with little net nuclear translocation, whereas the fast migration of an elongated and small nucleus coincided with effective nuclear translocation accompanied with little rotation.

Finally, we asked whether nuclear translocation and rotation originated in part from cell-to-cell variations or if a nucleus dynamically switched between these two modes of motion within the same cell. While carefully avoiding phototoxicity during long-term imaging of transfected cells, we monitored size, shape and centroid position of EGFP-histone H2B-labeled nuclei. We found that the nucleus was able to switch its migratory pattern dynamically between a translocation-dominated mode and a rotation-dominated mode during random cell migration (Fig. 2J and supplementary material Movie 6). Consistent with the previous result (Fig. 2C,D), quantitative analysis of single-nucleus tracking data confirmed the characteristic sigmoidal relationship between nuclear size and shape (Fig. 2K), which were inversely correlated with nuclear speed (Fig. 2L,M). Moreover, nuclear size increased with the magnitude of angular changes between consecutive centroid displacements of the nucleus (Fig. 2N).

Together, these results indicate that the nucleus of a migrating cell dynamically modifies its morphology and movement according to a tight relationship: the nucleus consistently becomes small and elongated when it moves rapidly and rotates little, and, vice versa, it becomes large and rounded when the nucleus moves slowly and mostly rotates.

The actin cap controls nuclear rotation and translocation

The actin cap tightly regulates nuclear shape in response to changes in cell shape (Khatau et al., 2009). Since the formation of the actin cap predicts both cell speed and persistence (Fig. 1) and the two modes of nuclear migration (i.e. translocation and rotation) are tightly related to nuclear morphology (Fig. 2), we asked whether nuclear translocation and rotation could be induced separately by controlling cell shape and migration. To study this, we placed cells both on fibronectin

Journal of Cell Science (2014) 127, 2528–2541 doi:10.1242/jcs.144345

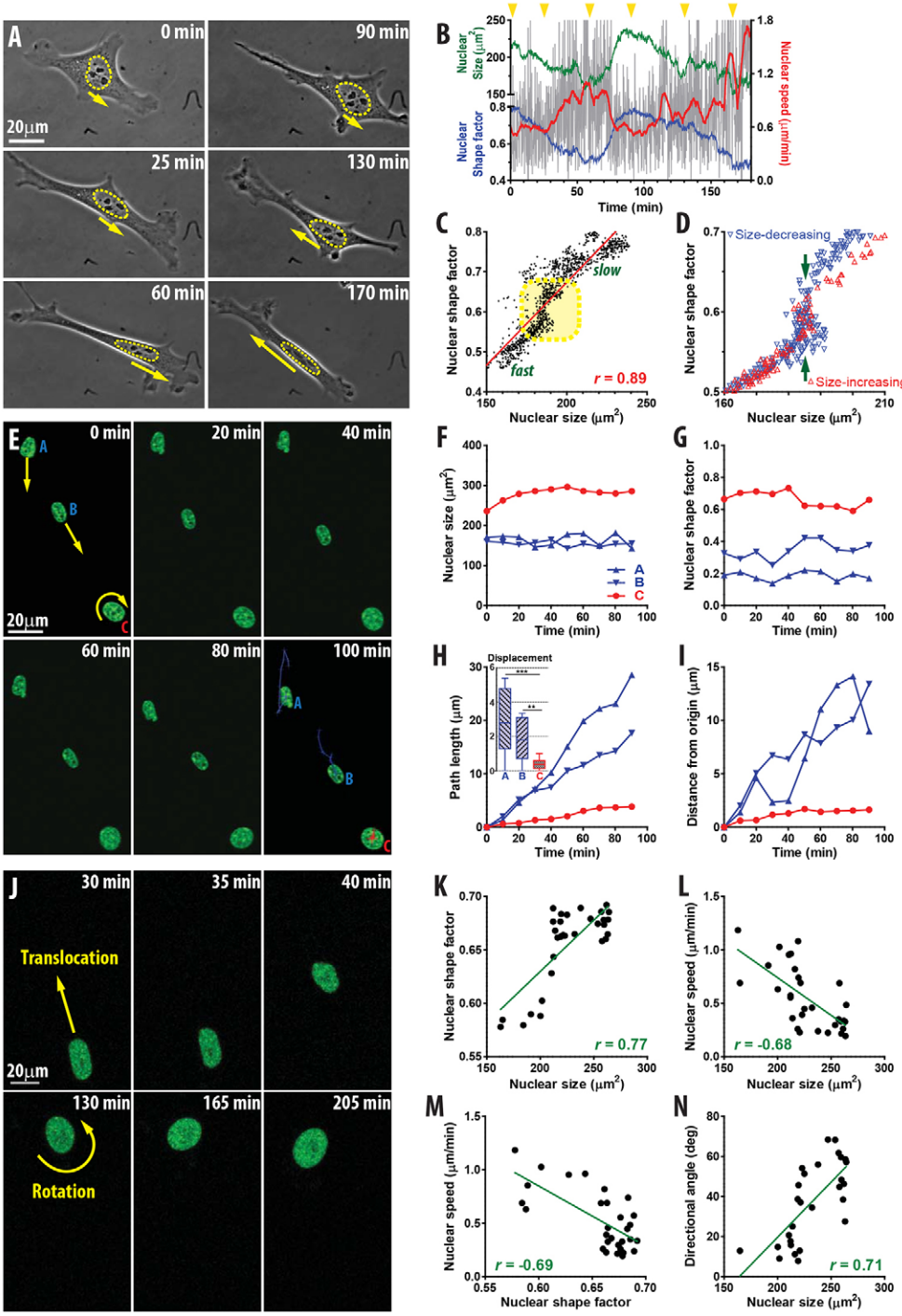

Fig. 2. See next page for legend.

microcontact-printed narrow stripes and circular islands. These adhesive patterns induced elongated and rounded cell shape, and mimicked the rapid persistent cell migration and slow non-persistent cell migration, respectively (Fig. 3A,B and supplementary material Movies 7 and 8), which naturally occur during regular random cell migration.

Nuclear morphology and organization of filamentous actin (F-actin) in cells plated on micropatterns were visualized under confocal laser microscope. By progressively lowering the focal plane from the apical surface of the cell to the underlying fluorescently labeled fibronectin patterns (Fig. 3A,B), we found that actin-cap stress fibers above the nucleus were consistently formed only for cells placed on stripe patterns (Fig. 3A,C), whereas the actin cap was consistently dismantled in cells placed on circular patterns (Fig. 3B,D). Importantly, basal actin stress fibers were similarly present in both conditions (Fig. 3A,B). Based on results in Fig. 2, we hypothesized that the nucleus of cells on circular patterns would show mostly rotation, whereas the nucleus of cells on stripes would show mostly translocation.

Journal of Cell Science (2014) 127, 2528–2541 doi:10.1242/jcs.144345

Fig. 2. Two distinct modes of nuclear migration. (A–D) Tight functional relationship between nuclear morphology and nuclear movements in a randomly migrating MEF. Dotted circles denote nuclear boundaries; length and direction of arrows represent nuclear speed and direction of movement, respectively, at the indicated time points (A). Morphometric analysis revealed dynamic changes in size, shape and speed of the nucleus (B). Nuclear size and shape were estimated by measuring the surface area (green) and shape factor (blue), defined as $4\pi A/P^2$, where A and P are the area and perimeter of the nucleus, respectively, approaching 1 for a perfectly round nucleus and 0 for a needle-like elongated nucleus. Nuclear speed (red) was estimated by measuring the centroid displacement of the nucleus every 10 s (gray), which was smoothed using a 2nd-order polynomial with four neighbors for each time point. Yellow arrowheads indicate corresponding time points captured in A. Changes in nuclear size and shape are synchronized and opposite to changes in nuclear speed (B). A nucleus became rounded as it increases in size, whereas the nucleus tends to move slowly (C). There is a distinct sigmoidal relationship between size and shape of the nucleus, as well as a strong positive correlation coefficient (r=0.89). The transition region (yellow dotted box) was re-plotted to distinguish the nuclear size-increasing phase (red triangles collected from 60~90 min) from the size-decreasing phase (blue inverted triangles collected from 0~60 min), where nucleus shape dramatically changed in a fixed nuclear size (~185 μm^2) and this change was detected both in the size-increasing phase and size-decreasing phase (D). (E–I) Movements of nuclei in MEFs transfected with EGFP-histone H2B. Two small and elongated nuclei (denoted by A and B) move more directionally than a large and rounded nucleus (denoted by C) that rotates clockwise in the same position (E). Nuclei were imaged every 10 min using time-lapse confocal microscopy. The size (F) and shape (G) of nuclei are closely related to the distinct displacement patterns. (H,I) Small and elongated nuclei move faster and farther than a large and rounded nucleus (A and B versus C). (J–N) Alteration of distinct nuclear migratory modes in the same nucleus. A EGFP-Histone H2B-tagged nucleus was monitored every 5 min (J). As shown above (A–D), as nuclear size increased, the nucleus tended to be round (K); this large and rounded nucleus moved slowly (L,M). Consistent with the above result (I), when the nucleus was small (and thus had an elongated shape), it moved more directionally (i.e. making less angular changes in direction of movement), whereas the nucleus could not maintain persistent motion when it became large (N). Pearson's correlation coefficients were estimated for each plot; the straight lines obtained by linear regression represent overall trends.

Cells confined to narrow stripes were elongated (Fig. 3G) and their nucleus maintained an elongated shape during one-dimensional cell migration (Fig. 3E,I and supplementary material Movie 7). By contrast, cells confined on circular adhesive islands were rounded (Fig. 3G) and did not undergo net migration whereas the periphery of these cells showed continuous formation and retraction of lamellipodial protrusions (Fig. 3F and supplementary material Movie 8). Quantitative analysis of DAPI-stained fluorescence micrographs indicated nuclei of elongated cells on the stripe patterns were smaller and more elongated than the nuclei of cells plated on the circular patterns (Fig. 3H,I). Analysis of live-cell movies showed that the nucleus of cells on stripes underwent rapid translocation and little rotation (Fig. 3J,K), whereas nuclei of cells on circular patterns displayed little translocation (Fig. 3J) but large rotational movements (defined as relative changes in angles computed from the centroid positions of nucleus and nucleoli), which produced significantly higher angular velocities than nuclei of cells on stripe patterns (Fig. 3K).

Together, these results indicate that the nucleus of cells on stripes and circular patterns undergo translocation and rotation, respectively, and exclusively of each other. These two distinct modes of nuclear motion are intimately related to the status of the actin cap and the movements of the cell: the nucleus mostly rotates when the actin cap is absent in slowly or non-moving rounded cells, whereas the nucleus mostly translocates when the actin cap is present in fast and persistently moving elongated cells.

Distinct nuclear movements synchronize with cell polarization

To induce actin-cap-mediated nuclear translocation and rotation separately, we used stripe-patterned cells that could move unidirectionally and round-patterned cells that were not motile. These are the phenotypic migrating modes of polarized motile cells and non-polarized non-motile cells, respectively (Petrie et al., 2009). Therefore, we asked whether the actin cap harnessed the cell polarity to differentiate two distinct nucleus/cell migratory modes.

As differentiated cells such as fibroblasts use microtubule-based cell polarity to establish their actin-rich leading edge to execute cell migration (Chung et al., 2000), we first monitored the random migration of EGFP-α-tubulin-transfected cells to visualize the microtubule network (Fig. 4A–C and supplementary material Movie 9). In contrast to the actin cap that showed distinct formation and disruption during nuclear translocation and rotation steps (Fig. 3), respectively, the overall organization of the microtubule network remained unchanged between these two steps (Fig. 4A–C). However, the nucleus and the centrosome (or microtubule-organizing center, MTOC) identified as the bright spot in these cells were differently located. Nuclei were located in the back of the cell and advanced forwards during nuclear translocation (supplementary material Fig. S3F), which was generally observed while cells moved persistently (i.e. fast migration), but they were located close to the centroid of the cell during nuclear rotation that was observed when cell migration was hindered and cells were repolarized for the subsequent persistent moves. When the elongated nucleus moved forward (translocation step, <30 min, Fig. 4B,C), the MTOC was positioned in the vicinity of the nucleus but away from the cell center (i.e. the cell was more polarized). By contrast, the MTOC was located inside the nuclear boundary and almost overlapped with the centroid of the cell (less polarized) when the elongated nucleus became rounded and nuclear rotation occurred (rotation step, >60 min, Fig. 4B,C).

Next, we quantitatively measured the relative positions of MTOC and nucleus in cells confined to stripes and circular islands (Fig. 4D–G), as these cells showed only nuclear translocation and nuclear rotation, respectively (Fig. 3). Previous studies reported that the centrosome in polarized motile cells is highly related to the directional cell migration but its location varies depending on cell type (Danowski et al., 2001; Desai et al., 2013; Niu et al., 1997; Pouthas et al., 2008; Ueda et al., 1997; Yvon et al., 2002), contact inhibition (Desai et al., 2013) and physical constraint (Jiang et al., 2005); our group recently demonstrated that MTOC position was highly correlated with cell polarization: the distance between MTOC and cell centroid was larger in polarized single cells (Hale et al., 2011). Consistent with the observation using EGFP-α-tubulin-transfected cells (Fig. 4A–C), the MTOC stained for γ-tubulin was away from the cell center, between the leading edge of the cell and the nucleus in the stripe-patterned cells, which is consistent with the direction of the cell migration, whereas it was localized close to the geometric centroid of the circular patterned cells (Fig. 4D–G).

These results further support our model of cell migration where the actin cap is the crucial regulator of the nucleus–cell-coupled

Journal of Cell Science (2014) 127, 2528–2541 doi:10.1242/jcs.144345

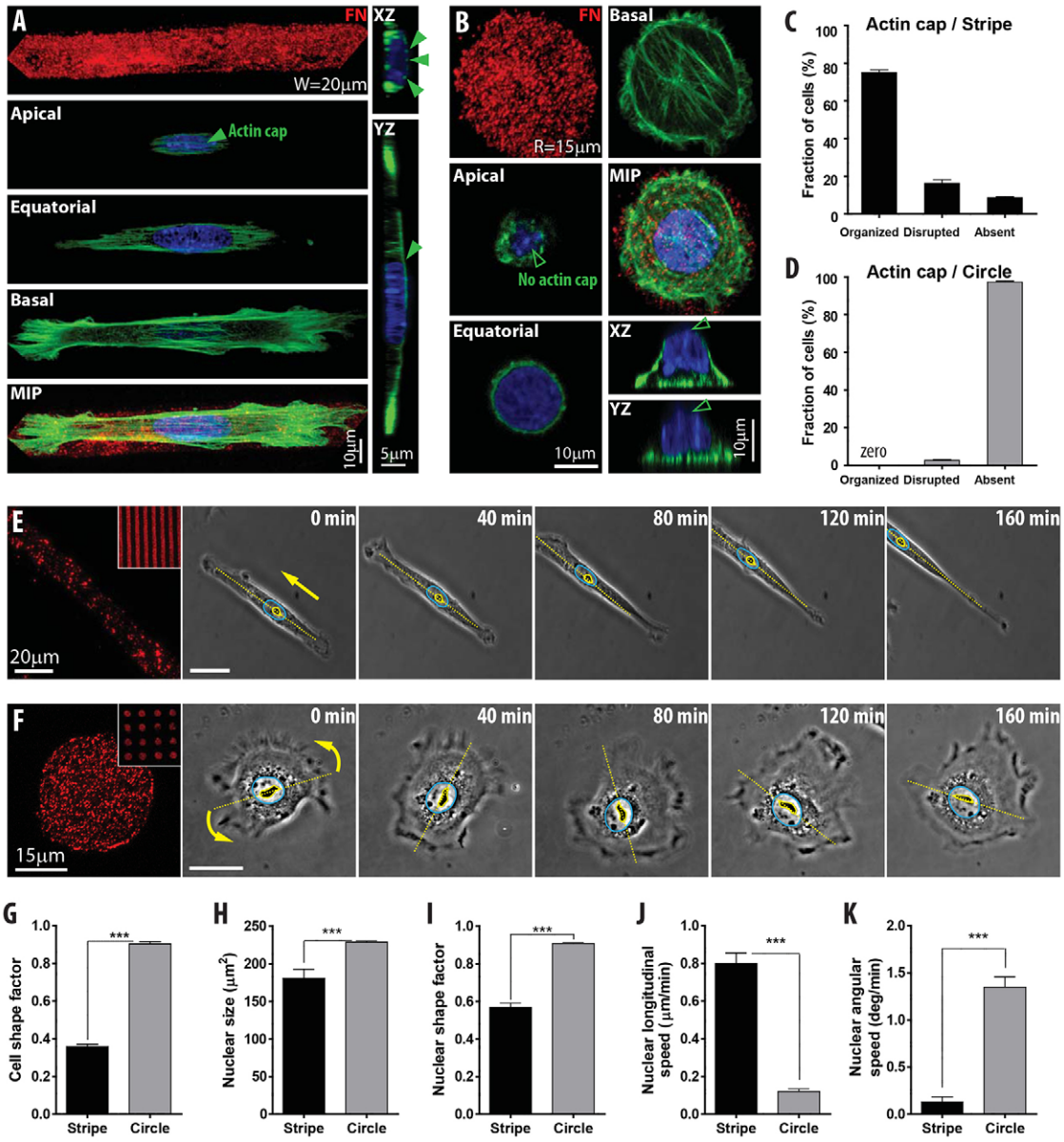

Fig. 3. Recapitulation of nuclear translocation and rotation. (A–D) Status of actin filaments in patterned cells. Actin filaments (green) and nucleus (blue) were visualized in cells on fibronectin-coated (FN, red) stripes (A) and circular patterns (B) via confocal microscopy. Focus on the apical plane of the nucleus revealed that aligned actin-cap fibers formed in stripe-patterned cells, whereas actin-cap fibers were absent in circular-patterned cells (A–D). Basal actin stress fibers were detected in both conditions. Three-dimensional reconstruction of confocal images shows actin-cap fibers aligned with the stripe direction (A). The nucleus covered by an actin cap in a stripe-patterned cell is more elongated (in *xy* plane) and thinner (in *z* direction) than the nucleus of a circular-patterned cell that does not form an actin cap (A,B). Full and open arrowheads indicate the presence and absence of actin-cap fibers, respectively. In C and D, over 250 cells were analyzed for each condition using three biological repeats. (E,F) Time-lapse monitoring of nuclear morphology and migration for cells confined to stripes and circular patterns. Elongated cells on stripe patterns moved directionally along the underlying stripes and nuclei only translocated without rotation (E), whereas rounded nuclei in cells on circular islands intermittently rotated with little net translocation (F). Width of stripe patterns and radius of circular patterns were 20 μm and 15 μm, respectively. Adhesive patterns were marked by a fibronectin primary antibody and Alexa Fluor 568-conjugated secondary antibody. Insets show low-magnification immunofluorescence images of micropatterns. Blue and yellow circles indicate the boundaries of the nucleus and one of its nucleoli (to quantify rotation), respectively, and the dotted line represents the long axis of the monitored nucleolus. (G–K) Quantification of the distinct cell shape, nuclear morphology and nuclear movement of cells plated on stripe and circular micropatterns. The cell body was highly elongated on the stripe patterns, whereas cells plated on the circular patterns were round (G). Cell shape factor was defined as W/L, where L is the longest chord of the cell and W is the caliper width, perpendicular to the length, approaching 1 for a less elongated and more symmetric cell shape and 0 for a unidirectionally elongated cell shape. Nuclei of cells confined to stripes were smaller (H), more elongated (I) and tended to move longitudinally faster (J) but rotated less (K) than nuclei in cells confined to circular patterns. In G–I over 100 DAPI- and actin-stained fixed cells were tested for each condition. In J and K, over 20 cells were analyzed for each condition.

migration, i.e. the presence of the actin cap mediates nuclear translocation and persistent directional cell migration by maintaining cell polarity, whereas the disruption of the actin cap deconstructs cell polarity and endows unpolarized cells with a chance to find a new direction to undergo their next persistent move.

Journal of Cell Science (2014) 127, 2528–2541 doi:10.1242/jcs.144345

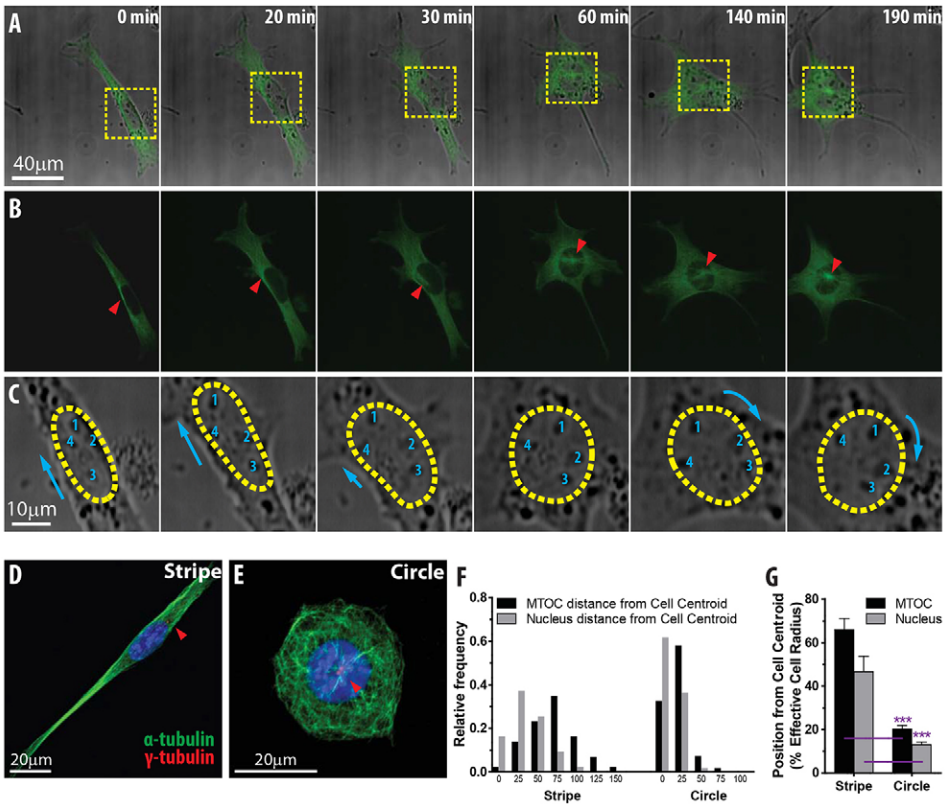

Fig. 4. Transition of cell polarization during cell migration. (A–C) The organization of the microtubules in a migrating cell. A cell transfected with EGFP-α-tubulin was monitored by time-lapse swept-field confocal microscopy. Maximum intensity projection of microtubule (green) and cell body (gray) are merged in the top panels (A) and GFP channel is extracted in the middle panels (B), where the position of the centrosome or MTOC was identified as a bright spot (red arrowheads). Nuclear morphology is enlarged in the bottom panels (C), where nucleoli and nuclear boundary are denoted by numbers (1–4) and dotted yellow circles and arrows indicate the nuclear motion. (D–G) Assessment of the cell polarity in distinct nucleus/cell migratory modes. Immunofluorescence of nucleus (blue), microtubule (green) and MTOC (red) stained by DAPI, α-tubulin and γ-tubulin, respectively, in cells plated on fibronectin-coated stripes (D) and circles (E). Frequency distribution of the relative distance (F) and averaged relative distance (G) of the MTOC (black) and nucleus (gray) from the centroid of the cell plated on adhesive stripes (left) and circles (right). Relative position was calculated from the effective cell radius. Over 50 cells were analyzed for each condition.

Lamin A/C and LINC complex-mediated differential formation of the actin cap regulates cell migration

We further validated our actin-cap-based model of nuclear migration by investigating the nuclear morphology and migratory mode in cells that naturally lacked an actin cap. The highly contractile fibers of the actin cap have previously been shown to shape the interphase nucleus through its dynamic connections to the LINC complexes and the nuclear lamina (Khatau et al., 2009). Our results in Figs 1 and 3 predict that the nucleus of cells lacking an actin cap should mostly undergo rotation and little translocation. As we have previously shown that lamin A/C deficiency disrupted the actin cap in MEFs (Khatau et al., 2009), we compared the nuclear morphology and movements of control and lamin A/C-deficient ($Lmna^{-/-}$) MEFs. $Lmna^{-/-}$ cells displayed a dismantled actin cap while the organization of basal actin fibers was mostly unchanged compared with control cells (Fig. 5A–D). The nucleus of $Lmna^{-/-}$ cells was also more rounded than the nucleus of control cells (Fig. 5E). Moreover, live-cell analysis revealed that the nucleus of actin-cap-forming control cells had a translocation speed that was twice as high as that of the nucleus of actin-cap-disrupted $Lmna^{-/-}$ cells (Fig. 5F; supplementary material Fig. S3G) and the nucleus of $Lmna^{-/-}$ cells rotated significantly more than the nucleus of control cells (Fig. 5G; supplementary material Fig. S3H).

Next, we analyzed the effect of lamin A/C deficiency on cell migration. Our results so far would predict that as the actin cap is disrupted in $Lmna^{-/-}$ cells (Fig. 5A–C), the overall cell speed and persistence should decrease (Fig. M–O) as nuclear translocation is decreased (Fig. 3). We measured the mean speed, final distance and mean persistence distance of control and $Lmna^{-/-}$ cells by tracking time-dependent centroid positions of individual cells. As predicted by our model of coupled cell-nucleus migration through the actin cap, both speed and persistence of $Lmna^{-/-}$ cells were diminished (Fig. 5H; supplementary material Fig. S3I,J), attenuating the ability of cells to spend long periods of time undergoing persistent migration before repolarization.

The various mechanical, pharmacological and genetic manipulations that we have discussed so far strongly support that the formation of the actin cap is highly relevant to fast persistent cell migration (Fig. 1), nuclear elongation and translocation (Figs 2 and 3), and cell polarization (Fig. 4). To further confirm the causality between the formation of an actin cap and cell migration, we assessed the migration of actin-cap-dismantled but -elongated cells. We first transfected cells with EGFP-KASH2 that significantly inhibited the formation of an actin cap and reduced persistent cell migration (Fig. 1I–O). Next, we confined these transfected cells onto the fibronectin-coated-stripes, where control cells formed an actin cap (>75%, Fig. 3C), their nuclei were elongated, longitudinal migration was dominant (Fig. 3I,J) and they readily moved persistently (Fig. 3E). Here, however, even though EGFP-KASH2-transfected cells maintained an elongated cell shape, the typical morphology of fast migrating cells (Fig. 5I,L), the actin cap was not organized (Fig. 5M) and their nuclei were not elongated but were round (Fig. 5I,N). This result is consistent with our previous results that demonstrated that the actin cap regulated nuclear shape in response to externally applied changes in cell shape (Khatau et al., 2009). Moreover, these cells lacking an actin cap, yet showing an elongated morphology, displayed significantly reduced cell migration compared with actin-cap-forming control cells, which moved unidirectionally along the underlying stripe patterns (Fig. 5J,K,O,P and supplementary material Movie 10). These results clearly verify that lamin A/C and LINC complexes

Journal of Cell Science (2014) 127, 2528–2541 doi:10.1242/jcs.144345

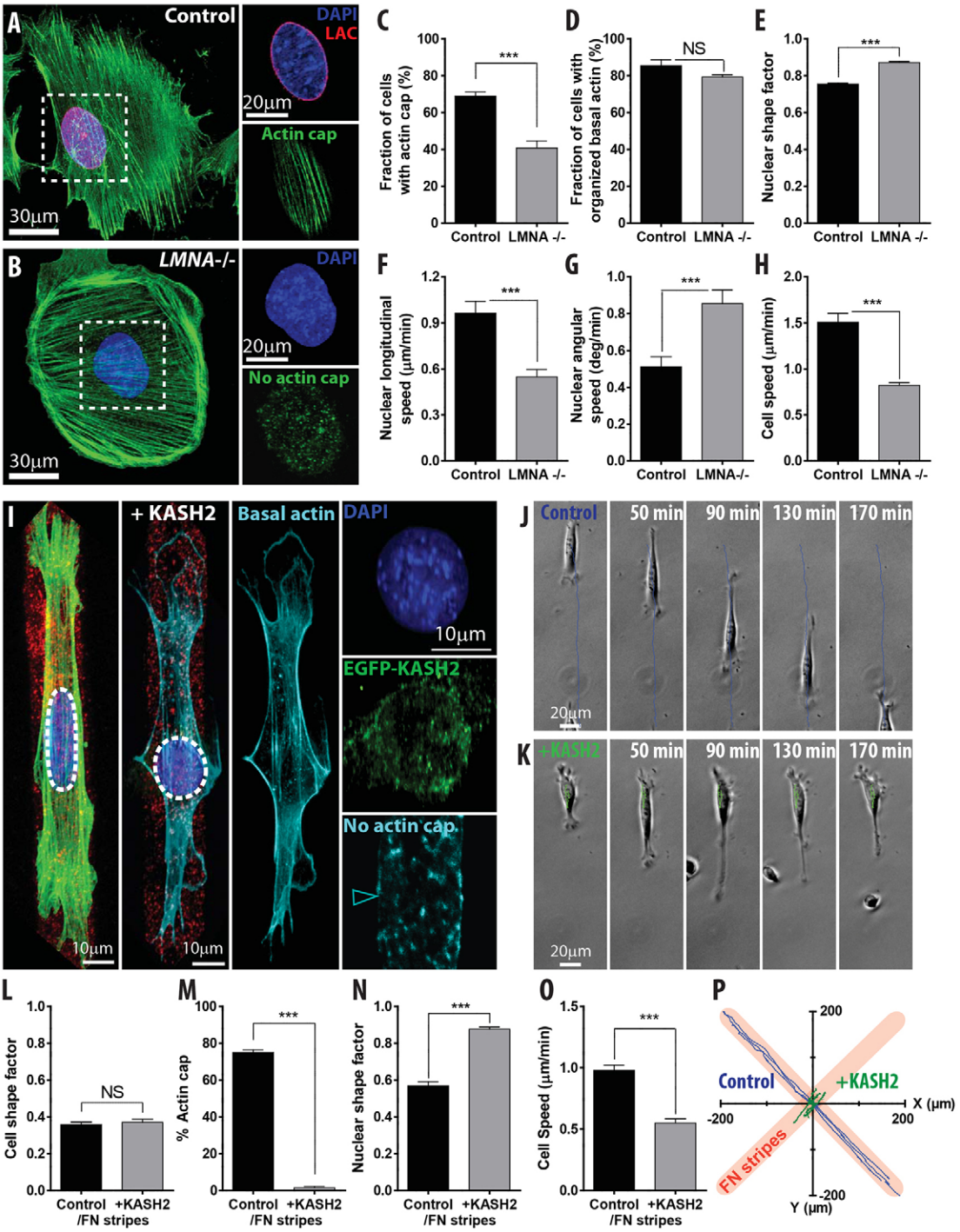

Fig. 5. Molecular mechanism controlling actin-cap-mediated coupled nucleus/cell migration. (A–E) Status of actin filaments and nuclear shape in control and lamin A/C-deficient (*Lmna*$^{-/-}$) cells. Representative organization of actin filaments and DAPI-stained nucleus were visualized by maximum-intensity projection in control (A) and *Lmna*$^{-/-}$ cells (B). Insets confirm that Lamin A/C (red) in the equatorial plane and well-organized actin-cap fibers on top of the nucleus formed only in control cells. Lamin A/C deficiency significantly reduced the fraction of cells forming an actin cap (C) without affecting basal actin structures (D), and increased nuclear shape factor (E). In C–E, over 300 cells were tested for each condition (five biological repeats for control and three for *Lmna*$^{-/-}$ cells). (F–H) Comparison of nuclear movement and cell migration between control and *Lmna*$^{-/-}$ cells. Lamin A/C deficiency significantly reduced nuclear translocation (F) but enhanced nuclear rotation (G), whereas cell speed decreased (H). In F and G, over 20 cells were analyzed; in H, over 50 cells were monitored per condition. (I–P) Verification of the role of actin cap in cell migration. Comparison of immunofluorescence of actin filaments (green or cyan), nucleus (blue) on fibronectin-stained adhesive stripes (red) between control (left) and EGFP-KASH2 (green) transfected cells (right). The image of the control cell is reused from Fig. 3A. EGFP-KASH2-transfected cells did not form an actin cap and showed round nuclear shape without affecting the organization of basal actin in the same micropatterns (I). Persistent migration of control (J) and impeded migration of EGFP-KASH2-transfected cells (K) on stripes. Quantification of cell shape (L), fraction of cells forming an organized actin cap (M), nuclear shape (N) and cell speed (O) show that the disruption of the actin cap prevents nuclear elongation and restricts cell migration in spite of elongated cell shape. Representative traces of migrating cells are depicted (P). EGFP-KASH2-transfected cells were identified using GFP channel before monitoring (K,O,P). In L–N, over 100 nuclei- and actin-stained cells were analyzed. In O,P, over 30 cells were monitored.

mediated coupled interplay between nucleus and cell through the actin cap, rather than through cell shape, and that this is crucial to direct persistent fast cell migration.

Dynein LIC2 drives nuclear rotation

To determine the molecular mechanism differentiating nuclear rotation from nuclear translocation, we analyzed nuclear motion in MEFs depleted of microtubule motor dynein. In particular, cytoplasmic dynein light intermediate chain 2 (LIC2) was depleted because this domain of dynein has been shown to be necessary for centrosomal localization (Schmoranzer et al., 2009), which determines the direction of moving cells (Ueda et al., 1997). We found no significant differences in the positions of the MTOC and the nucleus between control and LIC2-depleted cells (supplementary material Fig. S4), which was consistent with previous results the previous study that revealed that LIC2 was essential for neither single-cell polarization nor directional cell motility (Hale et al., 2011). Therefore, LIC2 does not dominate nuclear translocation that reflects polarized cell migration (Fig. 4), but it may play a role in nuclear rotation that occurs among the episodes of actin-cap-mediated nuclear translocation.

To confirm that LIC2 was necessary to drive nuclear rotation and determine how LIC2-mediated nuclear rotation was related to the formation of the actin cap, we compared the status of the actin cap, nuclear motion and cell migration in conditions that we have tested so far (Fig. 6). Compared with control cells that formed an actin cap and expressed LIC2 (Fig. 6A), cells specifically depleted of their actin cap through treatment with latrunculin B, transfection of the EGFP-KASH2 construct, deletion of *Lmna* and confinement on circular islands showed unchanged LIC2 distribution (Fig. 6B–E), diminished nuclear translocation accompanied by diminished cell speed, but enhanced nuclear rotation (green, Fig. 6I–L). By contrast, LIC2-depleted cells maintained an actin cap (Fig. 6F), but nuclear rotation was decreased threefold compared with control cells, while only marginally affecting nuclear translocation and cell migration (red, Fig. 6I–L). However, cells depleted of LIC2 and treated with latrunculin B (Fig. 6G) showed significantly decreased nuclear translocation and rotation (purple, Fig. 6I–K). Interestingly, contrary to latrunculin B-treated cells these latrunculin B-treated LIC2-depleted cells did not experience enhanced nuclear rotation compared with LIC2-depleted cells (Fig. 6K). These cells also showed significantly lower cell speed than either latrunculin B-treated cells or LIC2-depleted cells (Fig. 6l). Hence, nuclear rotation is driven by LIC2 but restricted by the actin cap and LIC2 does not regulate cell speed when the actin cap forms.

To reconfirm the LIC2-driven nuclear rotation further, we eliminated any possible interferences with the formation of actin cap or cell migration by placing LIC2-depleted cells on circular adhesive patterns (Fig. 6H), where no actin cap formed, no nuclear translocation was observed, and cell movements were completely confined (Fig. 6I,J,L and supplementary material Movie 11). Compared with the circular-patterned LIC2-expressing cells that showed the highest nuclear rotation, LIC2-depleted circular-patterned cells showed eightfold decreased nuclear rotation, which was a substantially larger decrease than the threefold decrease displayed by LIC2-depleted cells that formed an actin cap and could move as fast as control cells (Fig. 6K,L).

These results reinforced the notion that the actin cap is a crucial regulator of cell polarization and persistent cell migration as randomly migrating LIC2-depleted cells have the following features: (1) an actin cap was present (Fig. 6F,I); (2) the relative position of MTOC and nucleus remained intact (supplementary material Fig. S4); (3) nuclear translocation was maintained and only nuclear rotation was impeded (Fig. 6J,K); and (4) there was no significant changes in cell speed (Fig. 6L) or in persistence distance and persistence time (Hale et al., 2011). Therefore, LIC2-driven nuclear rotation is controlled by the actin cap: the actin cap obstructs nuclear rotation when it forms but allows nuclear rotation when it is disrupted (Fig. 6M). This further supports our hypothesis that the actin cap controls cell migration (Fig. 1): compare fast nuclear translocation in actin-cap-bearing fast-moving polarized cells with dominant LIC2-mediated nuclear rotation in slowly moving unpolarized cells that lack an actin cap.

Nuclear and cellular movements are coupled through the actin cap

Together, our results (Figs 1–6) suggest that the status of the actin cap predicts nuclear morphology (size and shape) and the type of nuclear movements (rotation versus translocation), as well as cell shape and the dominant mode of cell migration (fast persistent versus slow non-persistent). We now assess a possible interplay between nuclear and cellular movements through the actin cap in the same cell.

First, we monitored the formation and disruption of actin cap in EGFP-LifeAct-transfected live cells. In each time frame, confocal images from the top and bottom of the cell were collected to distinguish the actin cap in the apical region of the cell above the nucleus (red, Fig. 7A) from basal actin structures (green, Fig. 7A). As analyzed so far in fixed specimens, when the actin cap was removed from the top of the nucleus (between times ~460 min and ~510 min in Fig. 7A), nuclear translocation was switched to nuclear rotation and the cell changed its direction of movement (Fig. 7A and supplementary material Movie 12).

Next, we simultaneously monitored the nucleus, its nucleoli (to measure nuclear rotation), cell boundary and actin-cap fibers in EGFP-LifeAct-transfected cells (supplementary material Movie 13). The correlative analysis revealed that cell shape and cell speed were inversely related to nuclear morphology and modes of nuclear migration, respectively (Fig. 7B–E versus Fig. 7B,F–I). We next compared changes in cell shape and speed, nuclear morphology, nuclear longitudinal speed and angular speed with the status of actin-cap fibers in the same movies (Fig. 7J). Data were binarized so all measured quantities were either 0 or 1. In periods during which actin-cap fibers were present (yellow), a cell was elongated and moved rapidly, its nucleus was small and elongated, and nuclear translocation dominated, whereas in periods during which actin-cap fibers were dismantled (purple), the cell was rounded and moved slowly, its nucleus was large and rounded, and nuclear rotation dominated (Fig. 7J).

These results suggest that the intermittent stop-and-go motion of a cell during random migration is driven by the dynamic formation of the actin cap: during a persistent directional fast move, the cell is elongated and its small and elongated nucleus only translocates; during a phase where the cell does not significantly move, the cell is rounded and its rounded large nucleus only rotates to repolarize the cell for its next persistent directional move. This perpetual dynamic phenotypic switch is mediated by the dynamic formation of the actin cap (Fig. 7K).

Journal of Cell Science (2014) 127, 2528–2541 doi:10.1242/jcs.144345

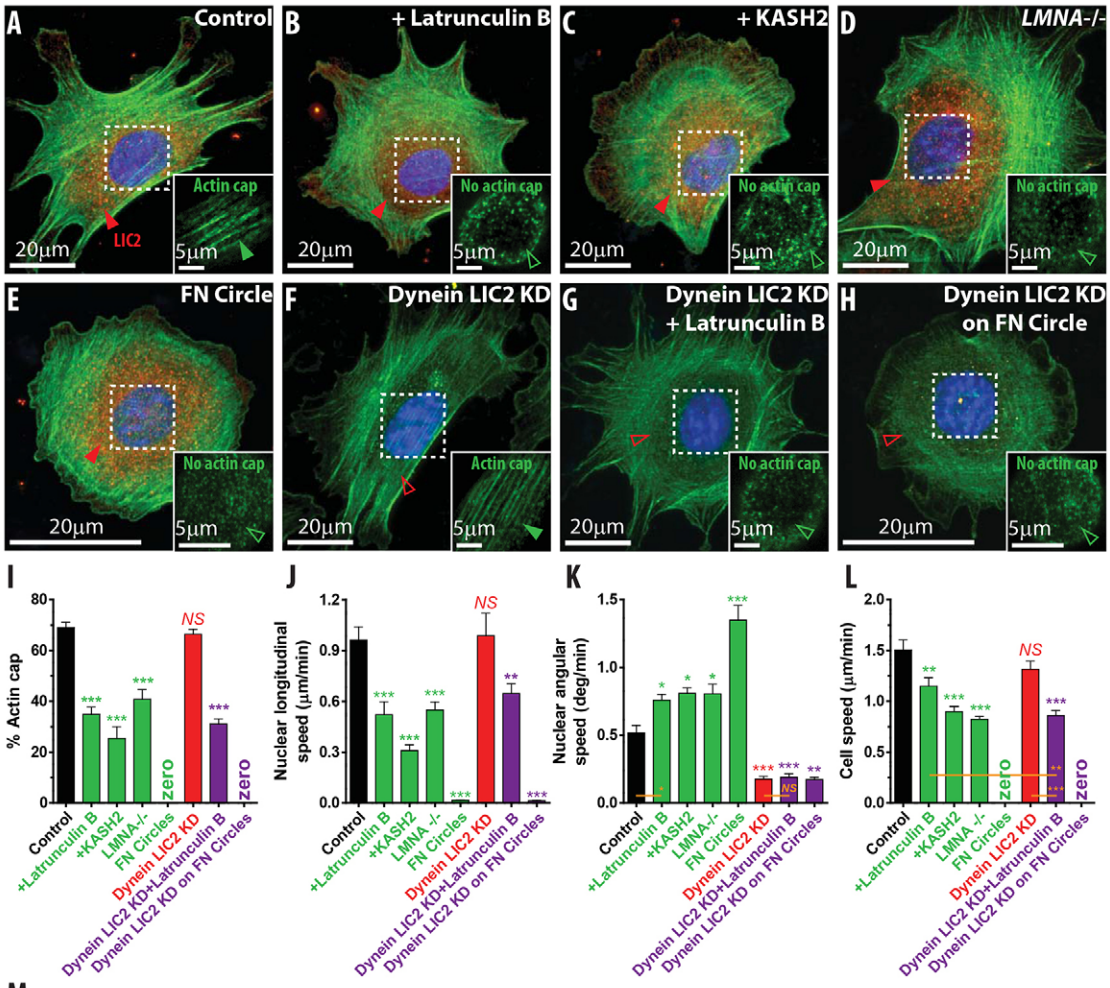

M

Condition	Actin cap	Dynein LIC2	Nuclear translocation	Nuclear rotation	Cell speed
Control	O	O	O	O	O
+Latrunculin B +KASH2 *LMNA*$^{-/-}$ FN Circles	X	O	---	+++	---
Dynein LIC2 KD	O	X	O	---	O
Dynein LIC2 KD +Latrunculin B Dynein LIC2 KD on FN Circles	X	X	---	---	---

+++ *Enhanced response*
--- *Reduced response*

Fig. 6. The role of LIC2 in nuclear rotation. (A–H) Organization of actin filaments (green) and LIC2 (red) of cells of control (A), cells treated with a low dose (60 nM) of latrunculin B (B), cells transfected with EGFP-KASH2 (C), cells originated from *Lmna*-deficient mice (D), cells plated on fibronectin (FN)-coated circular micropatterns (E), and cells depleted of LIC2 (F) and then treated with the same latrunculin B (G) or plated on the same circular islands (H). Closed and open red arrowheads indicate the presence (A–E) and absence (F–H) of LIC2, respectively. Insets depict the formation (closed arrowheads) or disruption (open arrowheads) of the actin cap. (I–L) Status of the actin cap, nuclear motion and cell migration. The fraction of cells forming actin cap (I), nuclear longitudinal speed (J), nuclear rotation speed (K) and cell speed (L) are differently colored: control, black; disruption of actin cap, green; depletion of LIC2, red; depletion of both actin cap and LIC2, purple. Over 300 cells were analyzed to determine the fraction of cells (I); over 20 cells were monitored every 5 min to measure nuclear migration (J,K); over 50 cells were monitored every 2 min for 8 h to measure cell motility (L). (M) Summary of nuclear motion and cell migration in response to the status of actin cap and LIC2. +++ and −−− depict the enhanced and reduced responses compared with control, respectively.

DISCUSSION

Our results establish a model of highly coupled migration between the cell and its nucleus mediated by the actin cap. Random migration of cells consists of the perpetual dynamic alternance of: (1) fast directional moves, accompanied by the translocation of the elongated actin-cap-bearing nucleus, which cannot rotate; and (2) low-speed ‘hesitation’ episodes between these directional moves, accompanied by LIC2-mediated rotation

Journal of Cell Science (2014) 127, 2528–2541 doi:10.1242/jcs.144345

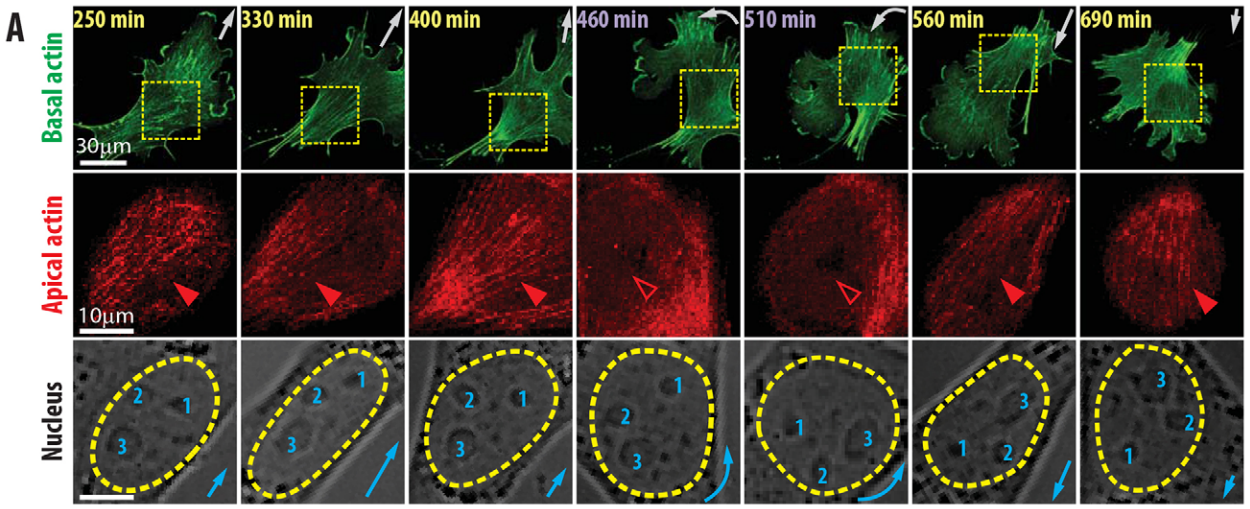

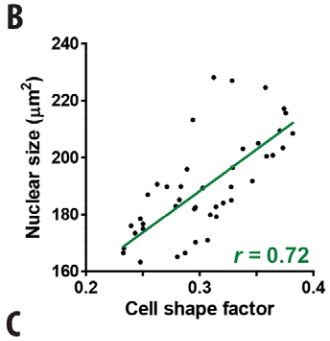

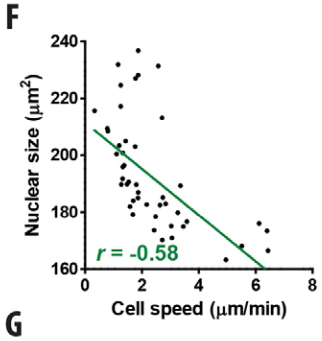

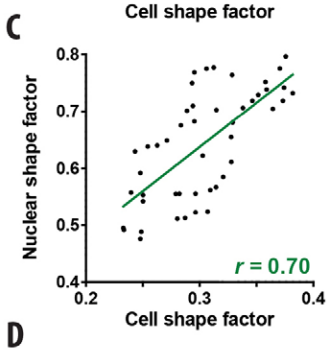

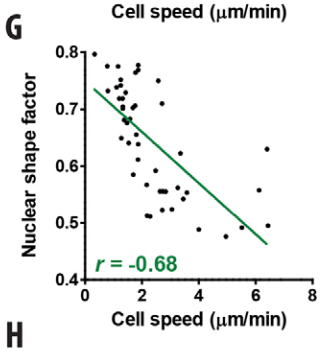

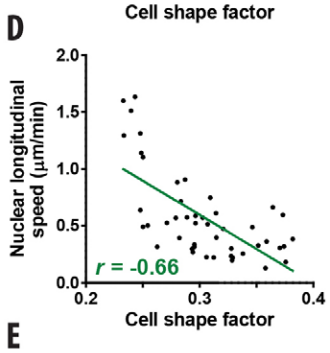

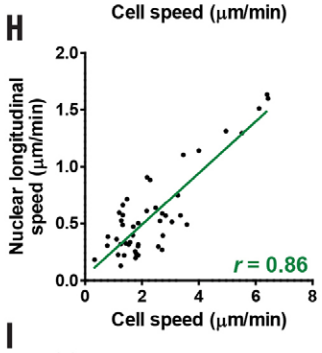

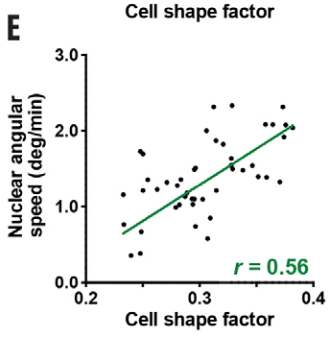

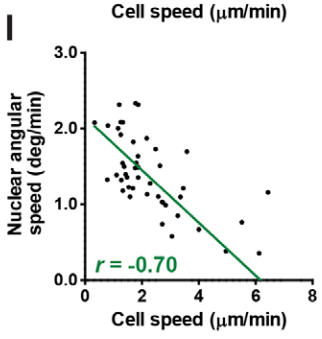

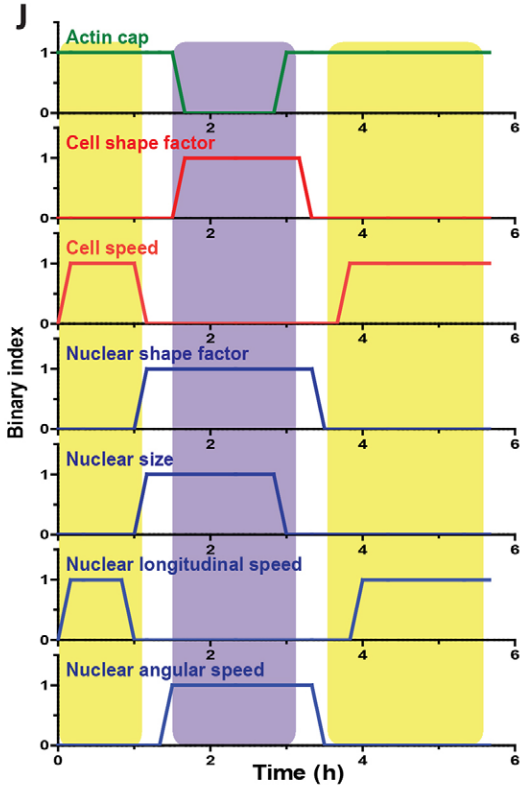

K

Summary		Actin cap	No actin cap
Nucleus	Morphology	**Elongated**	**Round**
	Migration	**Translocation**	**Rotation**
Cell	Morphology	**Elongated** *keeps polarization*	**Round** *breaks polarization*
	Migration	**Go** *persistent directional advance*	**Stop** *repolarization for redirection*

Fig. 7. See next page for legend.

Journal of Cell Science

Journal of Cell Science (2014) 127, 2528–2541 doi:10.1242/jcs.144345

Fig. 7. Multiparametric functional relationship between actin cap and dynamic changes of morphology and migration of nucleus and cell. (A) Actin cap in a live cell. EGFP-LifeAct-transfected MEF was monitored by time-lapse confocal microscopy. Distance from the top to the bottom of the cell is 6 μm; *z*-step was 0.25 μm. Images were captured every 10 min for ~12 h. Top 10 planes of collected images were maximum-intensity projected onto a single image to visualize the status of actin cap (red). Migrating direction of cell and nucleus is indicated in top and bottom panels, respectively. (B–I) Assessment of correlations among descriptors of cell morphology, cell migration, nuclear morphology and nuclear migration. As cell became rounded (i.e. increased cell shape factor), the nucleus increased in size (B) and became rounded (C), the longitudinal nuclear speed decreased (D) and the angular nuclear speed was high (E). As shape, size, migration speed of the nucleus oppositely responded to changes in cell shape and speed (B–E versus F–I), small and elongated nuclei were detected when cells moved rapidly (F,G) and thus longitudinal speed and angular speed of nuclei were correlated with cell speed positively (H) and negatively (I), respectively. In B–I, each data point was collected by monitoring a single cell every 5 min for 6 h. Pearson's correlation coefficients indicate the degree of correlation, while + and − indicate positive and negative correlations, respectively. The straight line in each plot obtained by linear regression was added to visualize overall trends. (J) Temporal changes in the status of actin cap (green), cell shape and speed (red), nuclear morphology and migration (blue) during the actin-cap-forming periods (yellow) and actin-cap-disrupted period (purple). In the presence of actin cap (yellow), the cell was elongated and moved fast, the nucleus was small and elongated, and nuclear translocation was dominant; in the absence of actin cap (purple), the cell was rounded and moved slowly, the nucleus was large and rounded, and nuclear rotation was dominant. In J, measurements used previously (B–I) were binarized by assigning 0 to values less than average or 1 to values greater than average. For the status of the actin cap, 0 corresponds to absence or disruption of the actin cap, while 1 corresponds to presence of organized actin-cap fibers. (K) Summary of actin-cap-mediated stop-and-go motion and corresponding interactions between nucleus and cell.

of the round, actin-cap-lacking nucleus that cannot translocate. During cell migration, the actin cap allows the cell to maintain a set polarization for a relatively long duration (30 min~2 h, Fig. 7J) before the cell can repolarize to re-orient in a new direction for its next persistent move. Hence, a cell undergoing persistent random-walk migration corresponds to a two-gear system tightly regulated by its actin cap.

Moreover, the focal adhesions that specifically terminate actin-cap fibers assist long-lived persistent moves of the cell. Unlike conventional focal adhesions that terminate regular stress fibers that are located over the entire basal surface of the cell, actin-cap-associated focal adhesions are specifically located at the two narrow sectors in the direction of the aligned actin-cap fibers, i.e. at leading lamellipodial edge and the trailing edge of the cell (Kim et al., 2012). As actin-cap-associated focal adhesions are significantly larger and longer-lived than conventional focal adhesions (Kim et al., 2012), these focal adhesions may stabilize and therefore define the principal lamellipodium, which allows long-lasting cell polarization and persistent cell migration in the direction of the actin-cap fibers.

Cell protrusions are continuously and dynamically generated along the entire periphery of adherent mesenchymal cells owing to actin assembly and to acto-myosin contractility. Our results suggest that most of these protrusions are short-lived because they are not stabilized by actin-cap-associated focal adhesions. Such short-lived side protrusions are readily observed in actin-cap disrupted cells (conditions in Fig. 6B–E). These protrusions cannot be stabilized by actin-cap-associated focal adhesions and, indeed, cell shape is more symmetric. These non-polarized, short-lived protrusions induce short-lived movements of the cell in haphazard directions, but no net cell movement as they cannot be turned into a polarized lamellipodium. In cases when the actin cap is disrupted, significant LIC2-driven nuclear rotation can occur because the brakes provided by the actin cap are off. This rotating nucleus in turn prevents stable polarization of the cell.

The actin cap can spontaneously disappear due to the finite lifetime of SUN-KASH binding at the nuclear envelope (Ostlund et al., 2009). We note that dual labeling of actin and focal adhesions in live cells reveals that the actin cap can naturally slide on the apical surface of the nucleus and fall to the bottom of the cell, instantaneously turning actin-cap fibers into regular basal stress fibers (Kim et al., 2012).Therefore, even cells that can have an actin cap (e.g. fibroblasts or endothelial cells), do not always display one. For example, at any time, only ~70% of MEFs show an actin cap (Fig. 1I). Such a highly dynamic feature of the actin cap may give rise to multiple possible interpretations about the role of the actin cap in nuclear motion. A recent study demonstrated that anterior actomyosin contraction was the driving force for the forward nuclear translocation, suggesting that the apical actin fibers (i.e. actin cap in our paper) were not necessary for this nuclear motion because nuclear translocation was observed while aligned apical fibers moved orthogonally or even while these fibers were stationary (Wu et al., 2014). Taking into account the dynamic assembly of LINC complexes that reorganize the actin cap in a highly dynamic manner, it may be possible to observe the lateral translation or stationary situation of actin-cap fibers, i.e. it is not necessary that the actin-cap fibers should move together with the nucleus, which also contradicts the highly dynamic LINC-mediated connections between the actin cap and nucleus. In our results, we demonstrate that the nuclear translocation (and correlated fast and persistent cell migration) was dominant in the actin-cap-bearing state and interpret as follows. Owing to the unique structure of the actin cap, the pulling force generated by the formation of new lamellipodia in the leading edge can be efficiently transmitted to the nucleus and the nucleus may advance through the continuous dynamic assembly and disassembly of LINC complexes, where actin-cap-associated focal adhesions may establish the principal lamellipodia in the direction of the actin-cap fibers, which determines the direction of cell migration.

In support of this model of nuclear migration controlled by coupled actin cap and dynein motor, we note that LIC2 does not regulate cell speed in the presence of an actin cap (Fig. 6L), whereas actin cap directs fast persistent cell migration (Fig. 1). When the actin cap dissolves, LIC2-mediated nuclear rotation becomes highly effective due to the absence of a physical obstacle (or brake), which allows cells to repolarize between persistent moves. Consistent with the previous study (Levy and Holzbaur, 2008) that demonstrated that dynein contributes to directed cell migration by maintaining nuclear centrality, dual elimination of the actin cap and LIC2 shows more significant reduction of cell migration than cells lacking an actin cap (but with active LIC2). Together, these results identify the role of LIC2-mediated nuclear rotation as the secondary driving force for directed cell migration when the actin cap disappears. When the actin cap is formed, the fibers of the actin cap constitute a natural barrier to nuclear rotation through LINC complexes, which span between the nuclear lamina and the actin cap, and may serve as a friction brake against LIC2-mediated nuclear rotation.

In this two-gear model of random cell migration, the forces of migration are still provided mostly by classical basal stress fibers, which are much more numerous than actin-cap fibers, whereas

the gearbox is the actin cap. When the actin cap is 'on', the cell moves fast and persistently; when the actin cap is 'off', the cell no longer moves efficiently.

MATERIALS AND METHODS

Cell culture

Control and lamin A/C-deficient (*Lmna*$^{-/-}$) mouse embryonic fibroblasts (MEFs) were cultured in Dulbecco's Modified Eagle's Medium (ATCC) supplemented with 10% fetal bovine serum (ATCC), 100 units/ml of penicillin and 100 µg/ml of streptomycin. To culture MEFs depleted of focal-adhesion proteins or LIC2, and C2C12 siRNA scramble and nesprin-2giant-depleted cells, 2 µg/ml and 10 µg/ml of puromycin were added into the culture medium, respectively, after selection. Reagents were purchased from Sigma unless stated otherwise.

Transient transfection and drug treatment

Transient transfection complex was prepared in Optim-MEM I reduced serum medium (Gibco) and FuGENE HD (Roche) according to the manufacturer's specifications. Latrunculin B was diluted to the final concentration of 60 nM. Cells were incubated with a drug added to the culture medium for 1 h before subsequent experiments.

Substrate preparation

Compliant polyacrylamide hydrogel (PAG) substrates were prepared by mixing acrylamide and N,N-methylenebisacrylamide in distilled H_2O at a final concentration of 5% and 0.15% (w/v). To initiate polymerization, ammonium persulfate and N,N,N′,N′-tetramethylethylenediamine (TEMED, Invitrogen) were introduced as 5% and 0.5% (v/v) of total mixture. The surface of the hydrogel was treated with UV-activatable cross-linker, N-Sulfosuccinimidyl-6-(4′-azido-2′-nitrophenylamino) hexanoate (sulfo-SANPAH, Pierce) before coating the 0.2 mg/ml type-I collagen (BD Biosciences). Unless stated, cells were plated on the same collagen-coated glass substrate.

Protein depletion

Depletion of focal adhesion proteins was conducted as described previously (Kim et al., 2012), where RNAi sequences targeting two different positions in mRNA of paxillin and zyxin were designed. After treating cells with lentiviral-mediated RNAi, cells showing >90% protein depletion efficiency were selected. To deplete LIC2, LIC2 sh116993 (5′-CCTCGACTTGTTGTATAAGTAC-3′) and LIC2 sh116996 (5′-GAAAGCCAGACTCTATGG TAAC-3′) were obtained from Sigma Aldrich. shRNA-induced protein knock-down was fully validated by western blots before use. Protein-depleted MEFs were selected in DMEM culture medium supplemented with 4 µg/ml puromycin for 3 days.

Fibronectin microcontact printing

Master micropatterns were created from custom masks as described previously (Khatau et al., 2009). PDMS (10:1 for base:curing agent, Corning) was poured over the master patterns and baked for at least 6 h at 60℃. Stamps were washed with ethanol and deionized water prior to each use. The PDMS stamps were incubated with protein solution of 50 µg/ml of fibronectin for 30 min. After removing the solution, stamps were air-dried and immediately placed onto the O_2 plasma-treated glass substrates to transfer patterns. After 1 min, the stamps were gently removed and glass substrates were washed with PBS and backfilled with 1 mg/ml polylysine-grafted polyethylene glycol (PLL-g-PEG, Susos AG, Switzerland) in a 10 nM HEPES solution for 10 min. Before plating cells, patterned substrates were soaked in medium and kept in the incubator for 30 min.

Immunofluorescence and confocal microscopy

Live-cell movies and immunofluorescence micrographs were collected using a Nikon A1 confocal laser scanning microscope equipped with a 60× oil-immersion objective (Nikon), a Nikon LiveScan swept-field confocal microscope with a 40×water-immersion or 100×oil-immersion objectives (Nikon), or a Cascade 1K CCD camera (Roper Scientific) mounted Nikon TE2000E epifluorescence microscope. To visualize actin filaments, vinculin-marked focal-adhesions and LIC2 cells were fixed with 4% paraformaldehyde. For staining α-tubulin and γ-tubulin, cells were fixed with methanol on the ice. Cells were permeabilized with 0.1% Triton and incubated with DAPI, Alexa Fluor phalloidin (Invitrogen), primary anti-vinculin (Sigma), anti-LIC (Abcam), anti-α-tubulin (Abcam) or anti-γ-tubulin (Abcam) antibodies for 1 h. To visualize nucleus and actin stress fibers in live cells, cells were transfected with EGFP-Histone H2B and EGFP-lifeact, respectively.

Motility and morphometric analysis

NIS elements (Nikon) and Metamorph (Molecular Devices) were used to analyze and process collected images. Morphometric measurement of nuclei (area and shape factor) was conducted using the image analysis software Metamorph offline (Molecular Devices). Centroid positions of nucleus and nucleoli were obtained by tracing them in each time frame and the nuclear rotational angle was calculated by the inner product of centroid-pointing vectors of nucleus and nucleolus, as described previously (Lee et al., 2005). To assess cell motility, x and y coordinates and time intervals were obtained by tracking single cells for 8 h. Cell speed was defined as mean displacement of centroid of individual cells calculated every 2 min of time interval. Final distance was defined as the end-to-end displacement that a cell made for 8 h and persistent distance was the mean distance that a cell traveled during a persistent move, which was defined as the traveling length ($\geq$10 µm) of a cell without making significant changes in direction of movement (>70°), as described previously (Kim and Wirtz, 2013a).

Microarray assay

Total RNA was prepared as described in the RNeasy Mini Kit (Qiagen) with on-column DNase I digestion. RNA quality was assessed by Nanodrp-1000 spectrometer for OD260/280 and OD260/230 ratio and Bioanalyzer (Agilent Technologies). MouseRef-8 v2 Expression BeadChip arrays (Illumina, San Diego, CA) were used for microarray hybridizations to examine the global gene expression of the samples. The array targets 18138 annotated mouse genes with 25697 unique probes derived from the National Center for Biotechnology Information Reference Sequence (NCBI RefSeq) database (Build 36, Release 22), supplemented with probes derived from the Mouse Exonic Evidence Based Oligonucleotide (MEEBO) set, as well as exemplar protein-coding sequences described in the RIKEN FANTOM2 database. Data were extracted with Gene Expression Module in GenomeStudio Software.

Statistics

All statistical analyses, including mean values, standard error of mean (s.e.m.), t-test and Pearson product moment correlation coefficient (r), were conducted using Graphpad Prism (Graphpad Software). Sample size was indicated in the figure caption. For the multiple comparisons between the control and all other conditions, Dunnett's post-hoc test was applied after one-way analysis of variance (ANOVA) with 95% confidence intervals (α=0.05). Error bars represent s.e.m. The significance between selected two conditions was determined by two-tailed unpaired Student's t tests: ***P<0.001, **P<0.01, *P<0.05 and NS for P>0.05.

Acknowledgements

The authors thank Sean X. Sun (Johns Hopkins University) for helpful discussions about the role of actin cap in cell migration; Dr Anjil Giri (Johns Hopkins University) for providing EGFP-α-Tubulin construct; Dr Gregory D. Longmore (Washington University in St Louis, School of Medicine) for providing their focal adhesion knockdown cells; and Dr Didier Hodzic (Washington University in St Louis, School of Medicine) for providing the C2C12 cell lines, anti-nesprin-2G antibody and EGFP-KASH constructs. Sample quality assessment and microarray analysis were conducted at the Sidney Kimmel Cancer Center Microarray Core Facility at Johns Hopkins University, supported by the National Institutes of Health [grant number P30 CA006973] entitled Regional Oncology Research Center.

Competing interests

The authors declare no competing interests.

Author contributions

D.K. designed, performed and analyzed all the experiments, and co-wrote the manuscript; S.C. helped with high-throughput image analysis; D.W. supervised the project and co-wrote the manuscript.

Funding

This work was supported by the National Institutes of Health (NIH) [grant numbers U54CA143868, R01CA174388]. Deposited in PMC for release after 12 months.

Supplementary material

Supplementary material available online at
http://jcs.biologists.org/lookup/suppl/doi:10.1242/jcs.144345/-/DC1

References

Berg, H. C. (1993). *Random Walks in Biology*. Princeton University, NJ: Princeton University Press.

Borrego-Pinto, J., Jegou, T., Osorio, D. S., Auradé, F., Gorjánácz, M., Koch, B., Mattaj, I. W. and Gomes, E. R. (2012). Samp1 is a component of TAN lines and is required for nuclear movement. *J. Cell Sci.* **125**, 1099-1105.

Bretscher, M. S. (2008). On the shape of migrating cells—a 'front-to-back' model. *J. Cell Sci.* **121**, 2625-2628.

Cadot, B., Gache, V., Vasyutina, E., Falcone, S., Birchmeier, C. and Gomes, E. R. (2012). Nuclear movement during myotube formation is microtubule and dynein dependent and is regulated by Cdc42, Par6 and Par3. *EMBO Rep.* **13**, 741-749.

Chaffer, C. L. and Weinberg, R. A. (2011). A perspective on cancer cell metastasis. *Science* **331**, 1559-1564.

Chung, C. Y., Lee, S., Briscoe, C., Ellsworth, C. and Firtel, R. A. (2000). Role of Rac in controlling the actin cytoskeleton and chemotaxis in motile cells. *Proc. Natl. Acad. Sci. USA* **97**, 5225-5230.

Danowski, B. A., Khodjakov, A. and Wadsworth, P. (2001). Centrosome behavior in motile HGF-treated PtK2 cells expressing GFP-gamma tubulin. *Cell Motil. Cytoskeleton* **50**, 59-68.

Desai, R. A., Gopal, S. B., Chen, S. and Chen, C. S. (2013). Contact inhibition of locomotion probabilities drive solitary versus collective cell migration. *J. R. Soc. Interface* **10**, 20130717.

Gomes, E. R., Jani, S. and Gundersen, G. G. (2005). Nuclear movement regulated by Cdc42, MRCK, myosin, and actin flow establishes MTOC polarization in migrating cells. *Cell* **121**, 451-463.

Gupta, G. P. and Massagué, J. (2006). Cancer metastasis: building a framework. *Cell* **127**, 679-695.

Hale, C. M., Chen, W. C., Khatau, S. B., Daniels, B. R., Lee, J. S. H. and Wirtz, D. (2011). SMRT analysis of MTOC and nuclear positioning reveals the role of EB1 and LIC1 in single-cell polarization. *J. Cell Sci.* **124**, 4267-4285.

Horwitz, R. and Webb, D. (2003). Cell migration. *Curr. Biol.* **13**, R756-R759.

Jiang, X., Bruzewicz, D. A., Wong, A. P., Piel, M. and Whitesides, G. M. (2005). Directing cell migration with asymmetric micropatterns. *Proc. Natl. Acad. Sci. USA* **102**, 975-978.

Khatau, S. B., Hale, C. M., Stewart-Hutchinson, P. J., Patel, M. S., Stewart, C. L., Searson, P. C., Hodzic, D. and Wirtz, D. (2009). A perinuclear actin cap regulates nuclear shape. *Proc. Natl. Acad. Sci. USA* **106**, 19017-19022.

Kim, D. H. and Wirtz, D. (2013a). Focal adhesion size uniquely predicts cell migration. *FASEB J.* **27**, 1351-1361.

Kim, D. H. and Wirtz, D. (2013b). Predicting how cells spread and migrate: focal adhesion size does matter. *Cell Adh. Migr.* **7**, 293-296.

Kim, D. H., Khatau, S. B., Feng, Y. F., Walcott, S., Sun, S. X., Longmore, G. D. and Wirtz, D. (2012). Actin cap associated focal adhesions and their distinct role in cellular mechanosensing. *Sci. Rep.* **2**, 555.

Kim, D. H., Chambliss, A. B. and Wirtz, D. (2013). The multi-faceted role of the actin cap in cellular mechanosensation and mechanotransduction. *Soft Matter* **9**, 5516-5523.

Köppen, M., Fernández, B. G., Carvalho, L., Jacinto, A. and Heisenberg, C. P. (2006). Coordinated cell-shape changes control epithelial movement in zebrafish and Drosophila. *Development* **133**, 2671-2681.

Lee, J. S. H., Chang, M. I., Tseng, Y. and Wirtz, D. (2005). Cdc42 mediates nucleus movement and MTOC polarization in Swiss 3T3 fibroblasts under mechanical shear stress. *Mol. Biol. Cell* **16**, 871-880.

Levy, J. R. and Holzbaur, E. L. F. (2008). Dynein drives nuclear rotation during forward progression of motile fibroblasts. *J. Cell Sci.* **121**, 3187-3195.

Li, R. and Gundersen, G. G. (2008). Beyond polymer polarity: how the cytoskeleton builds a polarized cell. *Nat. Rev. Mol. Cell Biol.* **9**, 860-873.

Luxton, G. W., Gomes, E. R., Folker, E. S., Vintinner, E. and Gundersen, G. G. (2010). Linear arrays of nuclear envelope proteins harness retrograde actin flow for nuclear movement. *Science* **329**, 956-959.

Morris, N. R. (2000). Nuclear migration. From fungi to the mammalian brain. *J. Cell Biol.* **148**, 1097-1102.

Niu, M. Y., Mills, J. C. and Nachmias, V. T. (1997). Development of polarity in human erythroleukemia cells: roles of membrane ruffling and the centrosome. *Cell Motil. Cytoskeleton* **36**, 203-215.

Ostlund, C., Folker, E. S., Choi, J. C., Gomes, E. R., Gundersen, G. G. and Worman, H. J. (2009). Dynamics and molecular interactions of linker of nucleoskeleton and cytoskeleton (LINC) complex proteins. *J. Cell Sci.* **122**, 4099-4108.

Petrie, R. J., Doyle, A. D. and Yamada, K. M. (2009). Random versus directionally persistent cell migration. *Nat. Rev. Mol. Cell Biol.* **10**, 538-549.

Pouthas, F., Girard, P., Lecaudey, V., Ly, T. B., Gilmour, D., Boulin, C., Pepperkok, R. and Reynaud, E. G. (2008). In migrating cells, the Golgi complex and the position of the centrosome depend on geometrical constraints of the substratum. *J. Cell Sci.* **121**, 2406-2414.

Schmoranzer, J., Fawcett, J. P., Segura, M., Tan, S., Vallee, R. B., Pawson, T. and Gundersen, G. G. (2009). Par3 and dynein associate to regulate local microtubule dynamics and centrosome orientation during migration. *Curr. Biol.* **19**, 1065-1074.

Starr, D. A. and Fridolfsson, H. N. (2010). Interactions between nuclei and the cytoskeleton are mediated by SUN-KASH nuclear-envelope bridges. *Annu. Rev. Cell Dev. Biol.* **26**, 421-444.

Stewart-Hutchinson, P. J., Hale, C. M., Wirtz, D. and Hodzic, D. (2008). Structural requirements for the assembly of LINC complexes and their function in cellular mechanical stiffness. *Exp. Cell Res.* **314**, 1892-1905.

Thiery, J. P., Acloque, H., Huang, R. Y. and Nieto, M. A. (2009). Epithelial-mesenchymal transitions in development and disease. *Cell* **139**, 871-890.

Ueda, M., Gräf, R., MacWilliams, H. K., Schliwa, M. and Euteneuer, U. (1997). Centrosome positioning and directionality of cell movements. *Proc. Natl. Acad. Sci. USA* **94**, 9674-9678.

Umeshima, H., Hirano, T. and Kengaku, M. (2007). Microtubule-based nuclear movement occurs independently of centrosome positioning in migrating neurons. *Proc. Natl. Acad. Sci. USA* **104**, 16182-16187.

Wilson, M. H. and Holzbaur, E. L. (2012). Opposing microtubule motors drive robust nuclear dynamics in developing muscle cells. *J. Cell Sci.* **125**, 4158-4169.

Wirtz, D., Konstantopoulos, K. and Searson, P. C. (2011). The physics of cancer: the role of physical interactions and mechanical forces in metastasis. *Nat. Rev. Cancer* **11**, 512-522.

Wu, J., Kent, I. A., Shekhar, N., Chancellor, T. J., Mendonca, A., Dickinson, R. B. and Lele, T. P. (2014). Actomyosin pulls to advance the nucleus in a migrating tissue cell. *Biophys. J.* **106**, 7-15.

Yvon, A. M., Walker, J. W., Danowski, B., Fagerstrom, C., Khodjakov, A. and Wadsworth, P. (2002). Centrosome reorientation in wound-edge cells is cell type specific. *Mol. Biol. Cell* **13**, 1871-1880.